Macroscopic behavior of bidisperse suspensions of noncolloidal particles in yield stress fluids

Thai-Son Vu, Guillaume Ovarlez and Xavier Chateau *

June 23, 2010

Synopsis

We study **both experimentally and theoretically the rheological behavior of isotropic bidisperse suspensions of noncolloidal particles in yield stress fluids. We focus on materials in which noncolloidal particles interact with the suspending fluid only through hydrodynamical interactions.** We observe that both the elastic modulus and yield stress of bidisperse suspensions are lower than those of monodisperse suspensions of same solid volume fraction. Moreover, we show that the dimensionless yield stress of such suspensions is linked to their dimensionless elastic modulus and to their solid volume fraction through the simple equation of Chateau *et al.* (2008). We also show that the effect of the particle size heterogeneity can be described by means of a packing model developed to estimate random loose packing of assemblies of dry particles. All these observations finally allow us to propose simple closed form estimates for both the elastic modulus and the yield stress of bidisperse suspensions: while the elastic modulus is a function of the reduced volume fraction ϕ/ϕ_m only, where ϕ_m is the estimated random loose packing, the yield stress is a function of both the volume fraction ϕ and the reduced volume fraction.

I   Introduction

Many industrial processes such as concrete casting, drilling muds, food-stuff transport ... and natural phenomena, such as slurries, lava flows ... involve suspensions of polydisperse particles suspended in a non-Newtonian fluid. Knowing and predicting the rheological properties of such suspensions is thus a major issue of both industrial materials mix design and science of deformation and flow of materials. For instance, it is well known that the grading of aggregate is

---

*Corresponding author; Electronic mail: xavier.chateau@lcpc.fr

one of the main factor influencing the hardened concrete strength; on the other hand, it has a large impact on the workability of concrete in its fresh state [Neville (1981)]. Consequently, a lot of work has been devoted to predict the influence of the particle size distribution on the concrete overall properties, both in the hardened and fresh state, and then to elaborate rational mix design methods [de Larrard (1999)]. As the rheological properties of a suspension (viscosity, yield stress, ...) are increasing functions of the solid particle volume fraction, it is necessary to lower this effect in order to design concrete mixtures containing the maximum amount of solid particles possible that can be transported, placed and finished easily. For this purpose, it is better to use aggregate with a distributed grading rather than particles of similar sizes.

The behavior of polydisperse, in particular bidisperse, Newtonian suspensions has received large interest from rheologists and several works, either theoretical or experimental, have been devoted to this subject in the last few decades. Different theoretical relationships aiming at predicting the viscosity of polydisperse suspensions as a function of the solid volume fraction ϕ and of the particle size distribution have been proposed in the literature [Farris (1968); Chong *et al.* (1971); Storms *et al.* (1990); Gondret and Petit (1997)]. In the three last works, the influence of the particle size distribution is taken into account through the concept of *maximum packing fraction* even if this concept is not always rigorously defined. It seems quite natural to define the maximum packing fraction of a suspension as the volume fraction for which the rheological properties tend to diverge. **Nevertheless, the determination of the value of the solid volume fraction at which the rheological properties diverge, and its link to packing models, pose problem.** In the case of monodisperse spheres, it seems to be equal to 0.57 for isotropic dispersions of particles [Mahaut *et al.* (2008a)], to 0.605 for anisotropic dispersions [Ovarlez *et al.* (2006)] while the random close packing of the dry particles is equal to 0.64.

Farris (1968) has investigated the relative viscosity of bimodal suspensions in the framework of a rigorous theoretical approach, valid only if the coarse particle size is much larger than the fine particle one (i.e. when λ, the coarse to fine particle ratio, is greater than 10). When this condition is fulfilled, one can consider that the coarse particles interact with the Newtonian fine particle suspension, and thence, the relative viscosity of the bimodal suspension is equal to the product of the relative viscosities of each monodisperse suspension. Of course, Farris approach can be generalized to polydisperse suspensions or to non-Newtonian suspending fluids provided that estimates of the monodisperse suspension's overall properties exist. Stovall *et al.* (1987) generalized Farris approach by taking into account interactions between the particles of different

size using the random close packing's model of Stovall *et al.* (1986) in order to address problems where scale separation between particles of different size is not possible. Nevertheless, it is believed that this work lacks of rigor because Farris reasoning is used by the authors in a situation where particle size separation is not possible. Later, Phan-Thien *et al.* (1997) developed a multiphase model for polydisperse suspensions. The idea consists in starting from the homogeneous linear suspending material (a Newtonian fluid or a Hookean solid) and in introducing the particles by infinitesimal volume fraction in the framework of an iterative process (differential scheme). The first step actually corresponds to the Einstein approach to the overall properties of a dilute suspension. Next steps consist in removing a small volume fraction of the suspending overall medium and in replacing it by the same volume of particles. Of course, such a process is rigorous only if particle size separation is possible at each step. Then, this model is only valid for the low solid volume fractions and hence is not applicable to concentrated suspensions. By the way, Phan-Thien *et al.* (1997) found that the values of the rheological properties estimated by this model are much smaller than those experimentally measured on polydisperse concentrated suspensions.

Besides theoretical works, experimental studies have also been performed. Shapiro and Probstein (1992), Probstein *et al.* (1994) and Chang and Powell (1994) used different types of viscometers to measure the steady viscosity of bidisperse suspensions. The same general trends are observed in these works. For a given value of the solid volume fraction, the viscosity of a bidisperse suspension is lower than the viscosity of a monodisperse suspension with same solid volume and the viscosity is a decreasing function of the maximum packing fraction of the particle size distribution. Interestingly, Chang and Powell (1994) also showed that the dimensionless viscosity $\eta(\phi)/\eta(0)$ of such suspensions is basically a function of ϕ/ϕ_m only, where ϕ is the particle volume fraction and ϕ_m is claimed to be the maximum packing fraction of the particle mixture. Gondret and Petit (1997) have measured the finite frequency viscosity of bidisperse suspensions. They also observed that the particle size distribution influences the dynamic viscosity of bidisperse suspensions, and that the lower maximum packing density distributions correspond to the lower dynamic viscosities.

>From these studies, it clearly appears that the viscosity of a polydisperse concentrated suspension is closely related to the maximum packing fraction of the suspended particles. Accordingly, the viscosity of a Newtonian suspension can be controlled by optimizing the particle size distribution [Servais *et al.* (2002)].

All these studies focused on the influence of the polydispersity on the viscosity of Newtonian suspensions while polydisperse non-Newtonian suspensions have been poorly studied. To our knowledge, this problem has been studied only by few authors and their studies provide extremely dispersed results. However, as explained in detail by Mahaut *et al.* (2008a) and Mahaut *et al.* (2008b), the data reported in these works do not correspond to homogeneous suspensions of particles interacting only mechanically with the suspending fluid, which is the subject we are interested in, and then are not applicable to a wide range of materials. **Geiker *et al.* (2002) studied experimentally the effect of coarse particles volume fraction on the rheological properties of self compacting concretes; they studied suspensions of polydisperse particles of various shapes but of same grading. They assumed that the effect of aggregates on fresh concrete rheological properties can be studied by looking to concrete as a suspension of coarse particles (the aggregates) in a yield stress fluid (the mortar): coarse particles interact only by non-Newtonian hydrodynamic forces. Both the fresh concrete and the mortar behaviors are described by a Bingham law. While Geiker *et al.* (2002) find that the dimensionless rheological properties for the different studied particles have very different shapes when plotted vs. the reduced volume fraction ϕ/ϕ_m, close examination of the results show that divergence actually occurs at different $\phi/\phi_m < 1$ for particles of different shape, in contradiction with the usual definition of the maximum packing fraction in rheology. In this study, ϕ_m was indeed defined as the random close packing of the dry granular assembly, which may not be relevant for comparing the rheological data. Moreover, the concrete was tested in a large gap coaxial cylinder rheometer and its rheological properties were estimated from the steady-state flow. It is well known that shear induced migration of particles is likely to occur in this situation [Ovarlez *et al.* (2006)]. Then, the tested materials may not be homogeneous when the system is at steady-state and it is not clear that the experimental data of Geiker *et al.* (2002) can be used to estimate the rheological properties of a well defined material (i.e. a material homogeneous at the coarse particles scale with a well defined distribution of particles within the tested volume). The fact that the yield stress estimates of Geiker *et al.* (2002) are much larger than estimates reported by other authors or in this work also casts doubt about the validity of their procedure.**

Ancey and Jorrot (2001) have experimentally studied the influence of adding

noncolloidal and non-Brownian particles within a clay dispersion on the value of the yield stress of the suspension. The ratio of the particle size was large enough so that the clay dispersion can be considered as homogeneous at the coarse particles scale. The authors have chosen to measure the yield stress of the suspension by means of a slump test in order to avoid the classical problems encountered with Couette rheometer (migration of particles, localization of the shear rate, anisotropy of the material) [Coussot (2005); Ovarlez *et al.* (2006)]. They showed that for well-graded materials, the monodisperse suspension yield stress does not depend on the particle characteristics (diameter, material) and that the relative yield stress diverges when the solid volume fraction value tends toward that of the maximum packing density. When the coarse particles are polydisperse, the value of the maximum packing density depends of the size distribution of the particles. Similarly to what is observed for Newtonian suspensions, the yield stress diverges for values of the solid volume fraction depending on the particle size distribution. The dimensionless yield stress $\tau_c(\phi)/\tau_c(0)$ measured for various mixtures of bidisperse particles then seem to collapse when plotted vs. the reduced volume fraction ϕ/ϕ_m. They also observed that for low reduced solid volume fraction, the yield stress can be a decreasing function of the solid volume fraction of the coarse particle. This effect was ascribed by the authors to a depletion phenomena. In the closeness of coarse particles, the clay particles are expelled from the suspending fluid. This effect induces an increase of the clay particle concentration far from the coarse particles which are embedded in a shell of viscous material (pure water) where the yield stress is naught. Then, the coarse particles can not contribute to the overall yield stress and behave as empty pores. Obviously, the observed decrease of the suspension yield stress originates from physicochemical effects. We recall that such effects are beyond the scope of this paper.

In this study, we are interested in situations where bidisperse mixtures of noncolloidal particles are dispersed in a yield stress fluid. It is recalled that yield stress fluids have a solid viscoelastic behavior below a yield stress; above this yield stress, they behave as liquids and their flow behavior is often well fitted to a Herschel-Bulkley law [Larson (1999)]. The influence of monodisperse particles on the behavior of yield stress fluid has been addressed experimentally by Mahaut *et al.* (2008a) and Mahaut *et al.* (2008b), and theoretically by Chateau *et al.* (2008).

The main result of these studies is that, when model materials are carefully designed to correspond to the theoretical case of homogeneous and isotropic distribution of monodisperse hard spheres interacting only mechanically through a yield stress fluid, there is a theoretical relationship linking the dimensionless linear properties of such suspensions to their nonlinear properties that is in very good agreement with the experimental data. As regards their elastoplastic properties, this relationship reads

$$\tau_c(\phi)/\tau_c(0) = \sqrt{(1-\phi)G'(\phi)/G'(0)}, \tag{1}$$

τ_c being the yield stress, G' the elastic modulus, and ϕ the particle volume fraction. They also observed that both the elastic modulus and yield stress are monotonically increasing functions of the solid volume fraction ϕ which seem to diverge when ϕ tends toward 0.57. Furthermore, their data are well fitted to a Krieger-Dougherty **like** equation

$$G'(\phi) = G'(0) \times (1 - \phi/\phi_m)^{-2.5\phi_m} \text{ with } \phi_m = 0.57 \tag{2}$$

and to its nonlinear generalization obtained by putting Eq. 2 into Eq. 1

$$\tau_c(\phi) = \tau_c(0) \times \sqrt{(1-\phi)(1-\phi/\phi_m)^{-2.5\phi_m}} \text{ with } \phi_m = 0.57 \tag{3}$$

In this work, we again restrict to situations where there is a scale separation between the paste microstructure and the noncolloidal particles in suspension and we focus on the purely mechanical contribution of the particles to the paste behavior. For this purpose, we use the experimental procedures described in Mahaut *et al.* (2008a). Accordingly, the experimental investigations reported in this paper focus on the behavior of the pastes in their solid regime, i.e., on the influence of particles on the elastic modulus and yield stress.

In Sec.II, we briefly present the materials employed and the experimental setup. Elastic modulus and yield stress measurements are shown in Sec. III. Then, in Sec. IV, we present a packing model and show that it allows to account for the dependence of the rheological properties on the particle mixture composition. Finally, in Sec.V, we combine the packing model estimates with the experimental data, and we demonstrate that it is possible to accurately predict the overall properties of the studied suspensions.
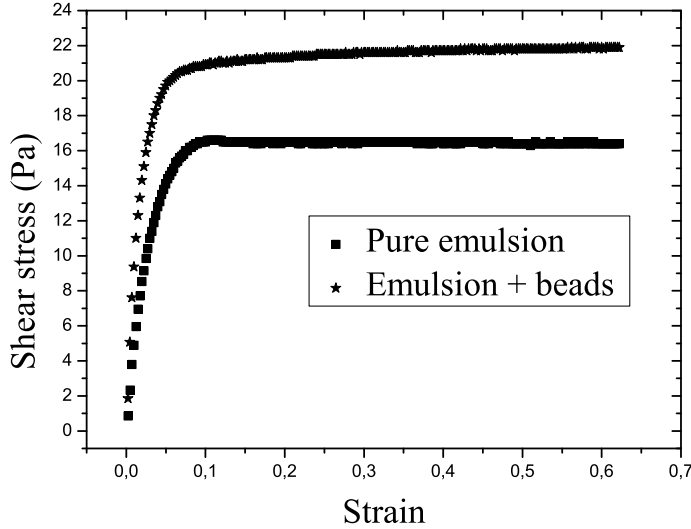
Figure 1: Shear stress vs strain when slowly shearing the material from rest at 10^{-2} s^{-1} for a pure emulsion (squares) and for a bidisperse suspension of 30% of 80 μm polystyrene beads mixed with 70% of 315 μm polystyrene beads with $\phi = 0.30$ in the same emulsion (stars).

II Materials and methods

In this section, we briefly present the main features of the suspensions we studied and of the experimental procedures we used for the elastic modulus and yield stress measurements. It is recalled that these procedures were designed to study the purely mechanical contribution of an isotropic distribution of particles to the yield stress fluid behavior. The interested reader is referred to [Mahaut *et al.* (2008a)] for a more detailed presentation.

A Materials

In order to evaluate the purely mechanical influence of the particles on the behavior of the paste, we designed materials to ensure scale separation between the matrix (the yield stress fluid) and the particles. We chose to use only inverse emulsions as a suspending fluid because Mahaut *et al.* (2008a) obtained the greater stability and the more reproducible results with this material in the monodisperse case. Moreover, the inverse emulsion behavior is very close to the ideal elastoplastic behavior of a yield stress fluid (see Fig. 1). The emulsion is a water-in-oil emulsion which microstructure scale is given by the droplets size, of order 1 μm from microscope observations. **As the continuous phase, we use a dodecane oil in which a Span 80**

7

emulsifier is dispersed at a 7% concentration. The dispersed phase is a 300 g/l CaCl2 solution dispersed in the oil phase at 6000 rpm for 1 h.

The particles are spherical beads. We used either polystyrene beads of density 1.05 g/cm^3, or glass beads of density 2.5 g/cm^3. We used bidisperse mixtures of polystyrene beads of diameter 80 μm and 315 μm (particle size ratio $\lambda = 3.94$) and bidisperse mixtures of glass beads of diameter 40 μm and 330 μm ($\lambda = 8.25$). The bimodal spherical beads are mixed together in the dry state. The particle mixture composition is defined by the fine particle proportion $\xi = V_{\mathrm{F}}/(V_{\mathrm{F}} + V_{\mathrm{C}})$ where V_{F} (resp. V_{C}) denotes the fine (resp. coarse) particle volume fraction. The particles are then dispersed in a volume V_ℓ of the suspending fluid so that their total volume fraction is $\phi = (V_{\mathrm{F}} + V_{\mathrm{C}})/(V_{\mathrm{F}} + V_{\mathrm{C}} + V_\ell)$. Finally, the fluid-particle mixture is stirred manually in random directions in order to homogenize it and obtain an isotropic material. In all cases, the paste yield stress was sufficient to avoid particle sedimentation in the solid regime. **The critical conditions for which a spherical object would fall under the action of gravity through a yield stress fluid at rest is obtained from the balance between the gravity force, the buoyancy and the drag force. A sphere of radius a immersed in a yield stress fluid with yield stress τ_c will not move under the action of gravity if $4/3(\rho - \rho_c)g\pi a^3$ is lower than $12k_c\pi a^3\tau_c$ with $k_c \simeq 3.5$, ρ_c the yield stress fluid density and g the gravity [Coussot (2005)]. In our experiments, the critical drag force is at least 30 times greater than the gravity force, which ensures stability at rest (thus for the elastic modulus measurements). When the suspension is sheared at low shear rate $\dot{\gamma}$, shear-induced sedimentation may occur with a velocity $V \approx 2/9(\rho - \rho_c)ga^2/(\tau_c/\dot{\gamma})$ [Ovarlez _et al._ (2010)]. Our yield stress measurements (see below) are performed at very low shear rate ($\dot{\gamma} = 0.01 s^{-1}$): this yields $V < 0.1\mu\mathrm{m.s}^{-1}$ for all the studied materials, i.e. shear-induced sedimentation can be considered as negligible over the duration of the experiments (less than 100 s).**

B   Rheological methods

The experiments were performed within a vane in cup geometry (inner diameter $d_i = 25$ mm, outer cylinder diameter $d_e = 36$ mm, height $H = 45$ mm) on a commercial rheometer (Bohlin C-VOR 2000). In order to prevent slippage at the walls, we used a six-blade vane as an inner tool immersed in a outer rough cylinder of roughness size equivalent to the size of the largest particles. We measured the elastic modulus $G'(\phi)$ through oscillatory shear experiments at a

single frequency in the linear regime, and the yield stress $\tau_c(\phi)$ through a single measurement at a small constant velocity ($\dot{\gamma} = 0.01 s^{-1}$) on each sample (see an example in Fig. 1). **The (static) yield stress is defined as the shear stress plateau in a shear stress vs. shear strain plot (Fig. 1). It is worth noting that we carefully checked that the same yield stress is measured whatever the (low) rotational velocity chosen to drive the inner tool is (i.e. $\dot{\gamma} \leq 0.01 s^{-1}$).** These methods where shown to provide fair estimates of the relative evolution of the elastic and yield stress properties with the particle volume fraction, and to ensure that the studied suspensions are isotropic and homogeneous [Mahaut *et al.* (2008a)].

III   Results

In this section, we present the elastic modulus and yield stress measurements performed on all the systems we studied, and compare the results to what was observed in monodisperse suspensions. Elastic modulus and yield stress measurements of various monodisperse suspensions of beads embedded in yield stress fluids were obtained by Mahaut *et al.* (2008a).

A   Elastic modulus measurement results

The results of the elastic modulus measurements performed on all the suspensions we designed are summarized in Tab. 1 and depicted in Fig. 2 as a function of the solid volume fraction ϕ. Two size ratio ($\lambda = 3.94$ and $\lambda = 8.25$) and several fine particle proportion values ξ were tested.

As classically observed for polydisperse viscous suspensions of different compositions, the experimental points do not fall onto a single curve. Nevertheless, we observe that the dimensionless elastic modulus is an increasing function of the solid volume fraction ϕ when λ and ξ are given. Moreover, all the data points for bidisperse suspensions fall below the law Eq. 2 valid for monodisperse suspensions. These results are perfectly consistent with the findings of the literature described in the introduction. It is also worth noting that all the experimental elastic modulus points fall above the Hashin-Shtrikman lower bound [Hashin and Shtrikman (1963)]:

$$G'(\phi)/G'(0) > (2 + 3\phi)/(2 - 2\phi) \tag{4}$$

which is a theoretical lower bound computed in the general case of a biphasic material (an infinitely rigid phase embedded in a linear elastic phase) isotropic both at the microscopic and the macroscopic scales.
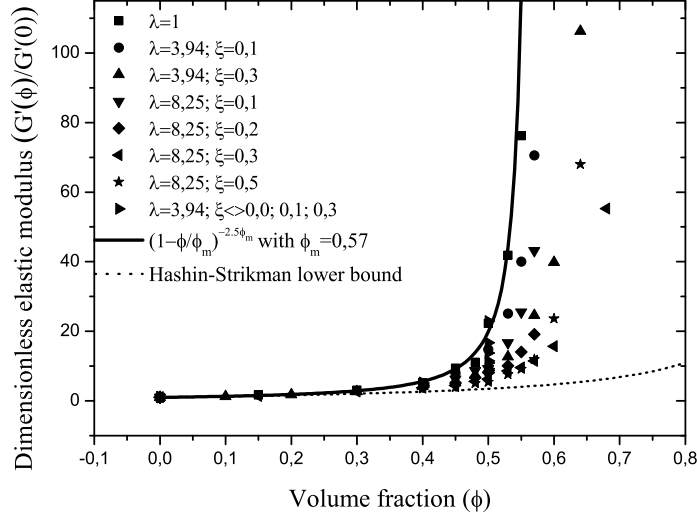
Figure 2: Dimensionless elastic modulus $G'(\phi, \lambda, \xi)/G'(0)$ as a function of the particle volume fraction ϕ for all the studied materials (**all particle size ratio λ and fine particle proportion ξ**). The solid line is the law Eq. 2. The dotted line is the Hashin-Shtrikman lower bound Eq. 4.

ϕ	$\lambda = 1.00$	$\lambda = 3.94$ $\xi = 0.1$	$\lambda = 3.94$ $\xi = 0.3$	$\lambda = 8.25$ $\xi = 0.1$	$\lambda = 8.25$ $\xi = 0.2$	$\lambda = 8.25$ $\xi = 0.3$	$\lambda = 8.25$ $\xi = 0.5$
0.00	1.00	1.00	1.00	1.00	1.00	1.00	1.00
0.10			1.27				
0.15	1.69		1.50			1.40	
0.20			1.79				
0.30	3.12		2.65			2.66	
0.40	5.19	4.68	4.13			3.78	
0.45	9.43	7.94	5.32	6.28	5.13	4.45	3.85
0.48	11.12	11.19	7.43	8.66	6.70	5.60	5.02
0.50	22.28	14.80	9.01	9.30	8.14	6.24	5.36
0.53	41.91	25.11	12.64	16.71	10.11	8.62	7.58
0.55	76.20	40.04	15.69	25.56	14.08	9.60	9.10
0.57		70.54	24.55	43.19	19.10	11.46	11.96
0.60			39.80	80.07	31.71	15.67	23.65
0.64			106.25		60.17	31.27	68.00
0.68						55.29	

Table 1: Dimensionless elastic modulus $G'(\phi, \lambda, \xi)/G'(0)$ as a function of the particle volume fraction ϕ for all the studied materials (**all particle size ratio λ and fine particle proportion ξ**).

ϕ	$\lambda = 1.00$	$\lambda = 3.94$ $\xi = 0.1$	$\lambda = 3.94$ $\xi = 0.3$	$\lambda = 8.25$ $\xi = 0.1$	$\lambda = 8.25$ $\xi = 0.2$	$\lambda = 8.25$ $\xi = 0.3$	$\lambda = 8.25$ $\xi = 0.5$
0.00	1.00	1.00	1.00	1.00	1.00	1.00	1.00
0.10			1.10				
0.15	1.11					1.11	
0.20			1.13				
0.30	1.26		1.32			1.31	
0.40	1.65		1.54			1.60	
0.45	2.26	1.68	1.73	1.75	1.73	1.69	1.69
0.48	2.87		2.16	1.94	1.65	1.99	1.74
0.50	3.53	2.45	2.35	2.32	2.03	2.01	1.94
0.53	5.32	2.81	2.91	3.26	2.16	2.24	2.10
0.55	8.00	4.27		4.23	2.43	2.41	2.54
0.57		6.13	4.06	5.34	2.77	2.81	2.59
0.60			4.58	5.96		3.26	5.07
0.64			7.30	11.72	7.21		9.06
0.68						5.64	

Table 2: Dimensionless yield stress $\tau_c(\phi, \lambda, \xi)/\tau_c(0)$ as a function of the particle volume fraction ϕ for all the studied materials (**all particle size ratio λ and fine particle proportion ξ**).

B Yield stress measurement results

We now present the results of the yield stress measurements performed on the different suspensions we studied. The experimental data are gathered in Tab. 2 and graphically represented in Fig. 3 as a function of the solid volume fraction ϕ.

The dimensionless yield stress exhibits the same trends as the dimensionless elastic modulus. It is an increasing function of the solid volume when the particle size ratio λ and the fine particle proportion ξ of the mixture are given. Moreover, similarly to what was observed for monodisperse suspensions [Mahaut *et al.* (2008a)], for a given particle mixture, the yield stress increase with the particle volume fraction is much lower than the elastic modulus increase.

IV Divergence of the rheological properties: The rigidity threshold of contact network

Although the data shown in Sec. III are scattered, we observe that all the G' and τ_c curves have basically the same shape and tend to diverge for a value ϕ_m of the volume fraction that seems to depend both on the size ratio λ and on the fine particle proportion ξ. As a first step towards the modelling of the rheological properties of the suspensions, it thus seems important to be able to predict the value of ϕ_m. This is the purpose of this section.
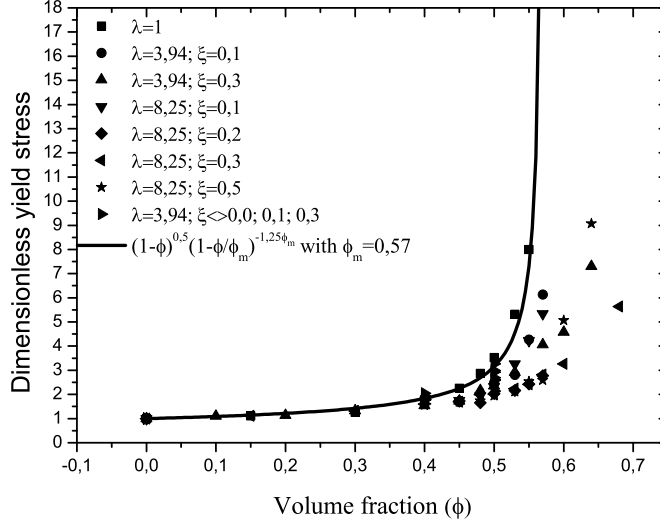
Figure 3: Dimensionless yield stress $\tau_c(\phi, \lambda, \xi)/\tau_c(0)$ as a function of the particle volume fraction ϕ for all the studied materials **(all particle size ratio λ and fine particle proportion ξ)**. The solid line represents the law $\tau_c(\phi) = \tau_c(0)\sqrt{(1-\phi)(1-\phi/\phi_m)^{-2.5\phi_m}}$ with $\phi_m = 0.57$ proposed by Chateau *et al.* (2008) for the monodisperse suspensions.

A   Packing model

Mahaut *et al.* (2008a) have shown that the elastic modulus G' of an isotropic suspension of monodisperse spherical beads is well fitted to the Krieger-Dougherty **like** law Eq. 2 with $\phi_m = 0.57$. **The quantity ϕ_m for which G' diverges is most probably no more than the contact rigidity threshold of the suspension: if $\phi < \phi_m$ the particles interact (hydrodynamically) through the suspending fluid. If $\phi \geq \phi_m$, the particles are close enough so that there is contact network spanning the whole material and that interparticle interactions (contact, friction, elasticity of the beads material ...) play a major role, leading to the apparent divergence of G'.** Interestingly, the overall yield stress of monodisperse suspensions also strongly increases when ϕ tends towards the same value $\phi_m = 0.57$.

At this stage, ϕ_m is just a fitting parameter. However, according to the observed trends of the overall properties of the bidisperse suspensions in Sec. IIIA and Sec. IIIB, there is strong evidence that this contact rigidity threshold is closely linked to the random close packing [Chang and Powell (1994); Gondret and Petit (1997); Probstein *et al.* (1994); Frankel and Acrivos (1967)]. This suggests to use packing models to predict how the value of the contact rigidity

12

threshold vary with the beads mixture composition. Furthermore, it is largely accepted that the packing density of an assembly of monodisperse beads depends upon the small gap inter-particle forces and the way the packing is produced. For example, Dong *et al.* (2006) obtained packing fractions ranging from 0 to 0.64 depending on the conditions between particles (0.64 for random close packing of frictionless cohesionless beads and 0 for random loose packing of beads involving strong van der Waals forces). When the cohesive forces between particles do not dominate over other forces, the random loose packing fraction, or more precisely, the sphere packing at its contact rigidity threshold ranges from 0.5 to 0.58 [Cumberland and Crawford (1987); Onoda and Liginer (1990); Dong *et al.* (2006)]. Then, the contact rigidity threshold $\phi_m = 0.57$ determined experimentally for monodisperse suspension, assuming it is representative of our mixture process, may be used as a fixed parameter of a packing model.

Various models have been proposed in the literature to address granular mixture problems. For a bidisperse beads mix, the packing density is a function of the particle size ratio λ, the fine particle proportion ξ and the way the packing was obtained [Ben Aïm and Le Goff (1967), Dodds (1980); de Larrard (1999)]. In most of the models of the literature, the packing process was taken into account through a scalar index. **In this work, we do not need to model the mixing process because we always used the same procedure to prepare the materials. We will first compute the value of the contact rigidity threshold of our bidisperse packings taking the monodisperse contact rigidity threshold ϕ_m as a free parameter; the value of ϕ_m will then be fixed in the sequel as the experimentally observed value 0.57 for our mixing process.** We chose to use the model of de Larrard (1999) which aims at taking the geometrical interactions between particles of different size into account. In this model, two different configurations of bidisperse mixtures are distinguished: dominant fine particle configuration when coarse particles are embedded in a fine particle matrix and dominant coarse particle configuration when fine particles fill the empty spaces between coarse particles. Furthermore, two geometrical interactions are taken into account:

Loosening effect : When one fine particle is inserted into a packing of coarse particles (which are thus dominant class) and if the fine particle is not small enough to locate in the empty space between the coarse particles, there is a loosening of the coarse particle packing which induces a decrease of the overall coarse particle density.

Wall effect : When one large particle is inserted into a local packing of fine particles (dominant

fine particle configuration), the fine particle density is decreased near the coarse particle. This wall effect induces a decrease of the overall fine particle density.

Bournonville *et al.* (2004) used a slightly modified version of the model of de Larrard (1999) to estimate the packing density of dry polydisperse beads mixtures. They showed that it is possible to directly use the experimentally measured packing density associated with the particular packing process used as a free parameter of the model. Moreover, they experimentally determined the function describing the loosening and wall effects described above. While they measured random close packing for monodisperse beads ranging from 0.59 to 0.62 for particles with diameters between 50μm and 320μm, we used exactly the same equations to estimate the divergence threshold of bidisperse suspensions, the only difference being the monodisperse threshold value. Since we are interested only in bidisperse mixtures, we only give the relationships allowing to estimate the contact rigidity threshold for such a suspension. The interested reader is referred to [de Larrard (1999); Bournonville *et al.* (2004)] for a more detailed review of the model.

To compute the contact rigidity threshold of a bidisperse mixture of particles of respective diameters d_{C} and d_{F} with $d_{\mathrm{C}} > d_{\mathrm{F}}$, one may first calculate the fine dominant particle density $\phi_m^{\mathrm{F\text{-}dom}}$ and the coarse dominant particle density $\phi_m^{\mathrm{C\text{-}dom}}$ defined by

$$\phi_m^{\mathrm{F\text{-}dom}} \quad = \quad \frac{\phi_m^{\mathrm{F}}}{1 - (1 - \xi)\left(1 - \phi_m^{\mathrm{F}} + b_{\mathrm{FC}}(\phi_m^{\mathrm{F}} - \frac{\phi_m^{\mathrm{F}}}{\phi_m^{\mathrm{C}}})\right)} \tag{5}$$

$$\phi_m^{\mathrm{C\text{-}dom}} \quad = \quad \frac{\phi_m^{\mathrm{C}}}{1 - \xi\left(1 - a_{\mathrm{CF}}\phi_m^{\mathrm{C}}/\phi_m^{\mathrm{F}}\right)} \tag{6}$$

where ϕ_m^{F} (resp. ϕ_m^{C}) denote the contact rigidity threshold of the monodisperse fine (resp. coarse) suspension, a_{CF} (resp. b_{FC}) a function describing the loosening (resp. wall) effect and ξ is the fine particle proportion defined above. In the sequel, we adopt $\phi_m^{\mathrm{C}} = \phi_m^{\mathrm{F}} = 0.57$ as determined experimentally by Mahaut *et al.* (2008a). The functions a_{CF} and b_{FC} were determined experimentally by Bournonville *et al.* (2004). They only depend upon the particle size ratio
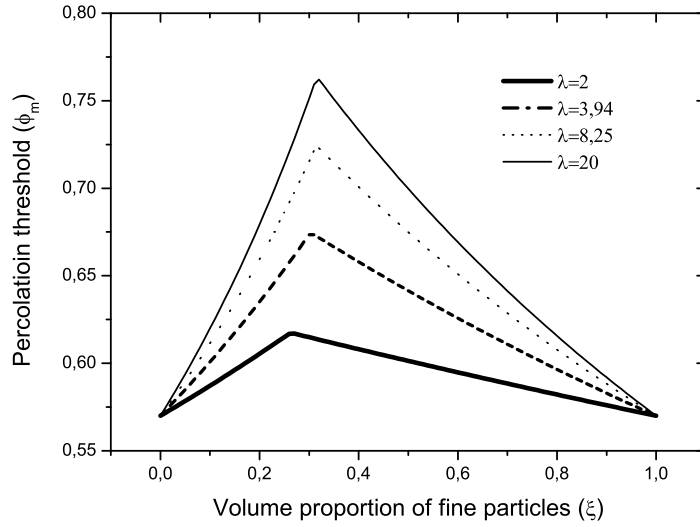
Figure 4: Contact Rigidity threshold ϕ_m of bidisperse suspensions as a function of the fine particle proportion ξ, for several size ratio $\lambda = 2$, $\lambda = 3.94$, $\lambda = 8.25$ and $\lambda = 20$.

$\lambda = d_c/ds$.

$$a_{\mathrm{CF}} = \left(1 - \left(1 - \frac{1}{\lambda}\right)^{1.13}\right)^{0.57} \tag{7}$$

$$b_{\mathrm{FC}} = \left(1 - \left(1 - \frac{1}{\lambda}\right)^{1.79}\right)^{0.82} \tag{8}$$

Finally, the bidisperse suspension contact rigidity threshold is defined by

$$\phi_m = \min(\phi_m^{\mathrm{C\text{-}dom}}, \phi_m^{\mathrm{F\text{-}dom}}) \tag{9}$$

Model predictions are shown in Fig. 4, where the contact rigidity threshold ϕ_m is plotted as a function of the fine particle proportion for several values of the size ratio λ.

Note that whatever the value of the size ratio, the maximum of the contact rigidity threshold is a singular point of the contact rigidity threshold versus fine particle proportion curve. Even if such a singular point was not experimentally observed for bidisperse packing of dry particles, it seems to be the hallmark of theoretical model distinguishing two regimes [Gondret and Petit (1997); de Larrard (1999)]. de Larrard (1999) corrected this undesirable effect by introducing a scalar index accounting for the packing process. Other models have been built to predict
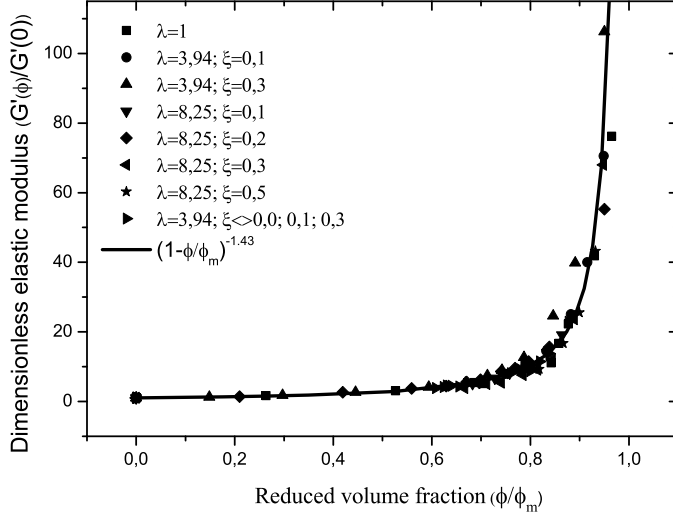
Figure 5: Dimensionless elastic modulus $G'(\phi, \lambda, \xi)/G'(0)$ as a function of the reduced solid volume fraction ϕ/ϕ_m for all bidisperse suspensions **(all particle size ratio λ and fine particle proportion ξ). The contact rigidity thresholds ϕ_m were calculated using the modified de Larrard model Eqs. 5 to 9.**

smooth variations of the packing density with respect to the fine particle proportion **[Gondret and Petit (1997)]. To our knowledge, it is not clear that smooth models are more accurate than non smooth ones. Furthermore, it will be shown in the sequel that Eqs. 5 to 9 are accurate enough to satisfactorily predict the influence of polydispersity onto both the elastic modulus and the yield stress of our suspensions. Then, the existence of this singular point seems to be a detail at this stage, and does not pose any problem in the framework of this study.**

B   Rheological properties vs Reduced solid volume fraction

In Sec. IV A, we have modelled the value of the contact rigidity threshold ϕ_m, i.e. the volume fraction for which the suspension rheological properties should diverge. We now propose to plot the dimensionless elastic moduli $G'(\phi, \lambda, \xi)/G'(0)$ and the dimensionless yield stress $\tau_c(\phi)/\tau_c(0)$ of all our bidisperse suspensions as a function of the predicted reduced solid volume fraction ϕ/ϕ_m. These data are presented in Fig. 5 and 6.

We first observe that, when plotted versus ϕ/ϕ_m, the dimensionless elastic modulus now falls onto a single master curve. **As the experimental data for monodisperse suspensions also**
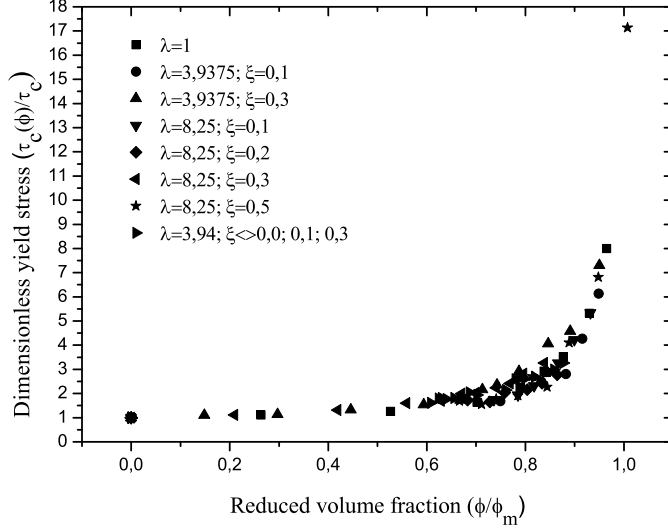
Figure 6: Dimensionless yield stress $\tau_c(\phi, \lambda, \xi)/\tau_c(0)$ vs the reduced beads volume fraction ϕ/ϕ_m for all bidisperse suspensions (**all particle size ratio λ and fine particle proportion ξ**). **The contact rigidity thresholds ϕ_m were calculated using the modified de Larrard model Eqs. 5 to 9.**

fall onto this curve, this curve should be fitted by a Krieger Dougherty like equation. This question is addressed in the sequel. It is not obvious that such a property holds for the dimensionless yield stress, even if the experimental data are less scaterred than when they are plotted as a function of the solid volume fraction. We observe that both the rheological properties tend to diverge for $\phi/\phi_m = 1$. This last observation is a strong indication that the packing model we use is able to predict correctly the impact of the particle size distribution on the value of the volume fraction for which the rheological properties diverge.

V   Analysis and discussion

In Sec. IV, we have shown that plotting the dimensionless rheological properties of bidisperse suspensions as a function of the reduced solid volume fraction ϕ/ϕ_m allows to obtain curves diverging when the reduced solid volume fraction tends toward 1. The purpose of the present section is to provide close-form estimates for the rheological properties of the bidisperse suspensions.

A   Elastic modulus

We have observed that dimensionless elastic moduli of all bidisperse suspensions plotted as a function of the reduced solid volume fraction ϕ/ϕ_m fall onto a single master curve. Then, by slightly modifying Eq. 2 so that the exponent does not depend on ϕ_m, we obtain a new estimate for the elastic modulus of bidisperse suspension

$$G'(\phi, \lambda, \xi)/G'(0) = (1 - \phi/\phi_m)^{-1.43} \tag{10}$$

which is shown as a solid line in Fig. 5. Satisfactorily, experimental data are very well fitted to Eq. 10. **As we have** $1.43 = 2.5 \times 0.57$ **for the exponent value in Eq. 10, the Krieger-Dougherty like Eq.10 agrees with Eq. 2.** However, even if a good agreement between the experimental data and the theoretical equation is obtained, it has to be noted that first order series expansion of Eq. 10 with respect to the variable ϕ yields the Einstein (1906) relation

$$G'(\phi\lambda, \xi)/G'(0) = 1 + 2.5\phi + O^2(\phi) \tag{11}$$

only for monodisperse suspensions, i.e. when $\phi_m = 0.57$. Discrepancy between estimates of the viscosity of concentrated suspension of solid particles and Einstein's equation is classical [Chang and Powell (1994); Frankel and Acrivos (1967)]. Eilers formula [Stickel and Powell (2005)] complies with both the Einstein equation and high concentration limit, but of course, this equation does not write as a single function of the normalized solid volume fraction ϕ/ϕ_m because Eq. 11 does not. As our experimental data are well fitted to the closed form estimate Eq. 10, we leave this problem aside in this work.

In Fig. 7, we plot the experimentally measured dimensionless elastic moduli $G'(\phi\lambda, \xi)/G'(0)$ as a function of the fine grain proportion ξ, for fixed size ratio $\lambda = 3.94$, for two solid volume fraction $\phi = 0.4$ and $\phi = 0.5$. These experimental data are gathered in Tab. 3.

Experimental $G'(\phi\lambda, \xi)/G'(0)$ shows a minimum at a value of ξ close to 0.40. This minimum should thus correspond to the optimal mixture of particles of size ratio $\lambda = 3.94$. The experimental data are also compared with Eq. 10 in Fig. 7, the contact rigidity thresholds being computed thanks to the model presented in Sec. IV.

The agreement between the experimental data and Eq. 10 is rather good meaning that the granular packing model combined with the elastic Krieger-Dougherty equation capture the essen-
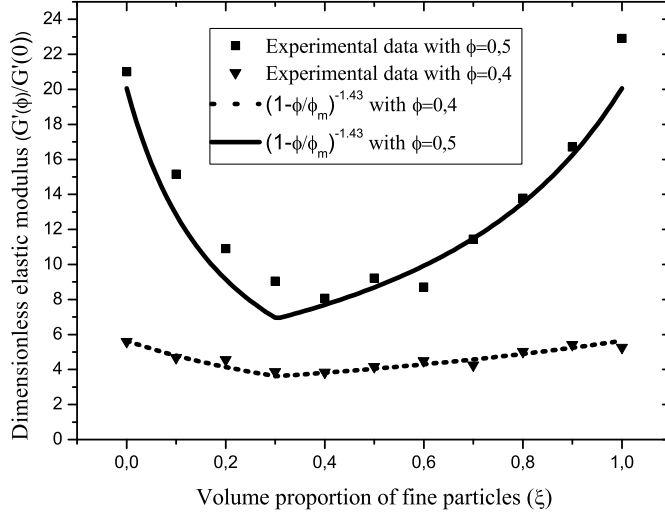
Figure 7: Dimensionless elastic modulus $G'(\phi, \lambda, \xi)/G'(0)$ vs fine particle proportion ξ for suspensions of 80 μm and 315 μm polystyrene beads with solid volume fraction $\phi = 0.4$ (filled triangle) and $\phi = 0.5$ (filled square). The dot (resp. solid) line is Eq. 10 computed for $\phi = 0.4$ (resp. $\phi = 0.5$). The contact rigidity thresholds ϕ_m were calculated using the modified de Larrard model Eqs. 5 to 9.

tial features of the studied system. However, the theoretical dimensionless elastic modulus has a minimum at $\xi = 0.30$ while the smallest elastic modulus was measured for suspension with ξ close to 0.4. This discrepancy possibly comes from the packing model which was validated on dry beads packing experiments, whereas beads are suspended in a fluid in this work. Finally, close inspection of the data suggest that the dimensionless elastic modulus vs fine particle proportion curve is smooth while the tangent to the theoretical curve is discontinuous at the point where $G'(\phi, \lambda, \xi)/G'(0)$ reaches its minimal value. As pointed out in Sec. IV, this singularity in the theoretical curve clearly originates from the packing model. Even if the packing model could be improved to obtain smooth theoretical curves, it is believed that the model used in this work is accurate enough given the dispersion of experimental data.

B Elastic modulus vs yield stress

Proposing estimates for the overall properties of a suspension of particles dispersed in a non-Newtonian fluid is challenging. However, Chateau $et\ al.$ (2008) have recently shown that it is possible to relate the overall yield stress of a suspension of particles isotropically dispersed in a yield stress fluid to its overall elastic modulus in its solid regime, provided that the heterogeneities

Elastic Modulus	$\phi = 0.4$	$\phi = 0.5$		Yield stress	$\phi = 0.4$	$\phi = 0.5$
$\xi = 0.0$	5.60	21.01		$\xi = 0.0$	1.91	3.33
$\xi = 0.1$	4.68	15.16		$\xi = 0.1$	1.84	2.93
$\xi = 0.2$	4.56	10.90		$\xi = 0.2$	1.81	2.61
$\xi = 0.3$	3.87	9.05		$\xi = 0.3$	1.94	2.33
$\xi = 0.4$	3.84	8.07		$\xi = 0.4$	1.61	2.14
$\xi = 0.5$	4.16	9.23		$\xi = 0.5$	1.79	2.58
$\xi = 0.6$	4.51	8.71		$\xi = 0.6$	1.77	2.62
$\xi = 0.7$	4.25	11.45		$\xi = 0.7$	1.81	2.69
$\xi = 0.8$	5.03	13.78		$\xi = 0.8$	1.80	2.92
$\xi = 0.9$	5.43	16.71		$\xi = 0.9$	2.04	2.99
$\xi = 1.0$	5.26	22.91		$\xi = 1.0$	1.94	3.26

Table 3: Dimensionless elastic modulus $G'(\phi, \lambda, \xi)/G'(0)$ and dimensionless yield $\tau_c(\phi, \lambda, \xi)/\tau_c(0)$ stress as a function of the fine particle proportion ξ, for particle size ratio $\lambda = 3.94$.

of the strain rate field over the suspending fluid domain can be neglected (see Eq. 1). To obtain this relationship, it was assumed that the particles are rigid, noncolloidal and that there are no physicochemical interactions between the particles and the paste. It is recalled that our experimental procedure was designed to fulfill all these hypotheses [Mahaut *et al.* (2008a)]. **In this case, the apparent viscosity $\eta^{\mathbf{app}}$ of the suspension sheared at a macroscopic shear rate $\dot{\gamma}$ reads**

$$\eta^{\mathbf{app}}(\phi, \dot{\gamma}) = \frac{G(\phi)}{G(0)} \times \eta_0^{\mathbf{app}}(\dot{\gamma}_{\mathbf{eff}}) \tag{12}$$

where $\eta_0^{\mathbf{app}}$ is the apparent viscosity of the suspending fluid sheared at an effective strain rate $\dot{\gamma}_{\mathbf{eff}}$ that accounts for the shear rate locally experienced by the pure suspending fluid, and $G(\phi)$ is the elastic modulus of the same suspension of particles (i.e. same size and same position) dispersed in an elastic material. Eq. 12 simply says that in a nonlinear (non-Newtonian) medium, the viscosity increase of the suspension with the particle volume fraction ϕ is simply the same as in a linear (Newtonian or elastic) medium whose viscosity would be the apparent viscosity $\eta_0^{\mathbf{app}}(\dot{\gamma}_{\mathbf{eff}})$ of the sheared suspending fluid; in this case, an additional dependence of the apparent viscosity on ϕ comes from the $\dot{\gamma}_{\mathbf{eff}}$ dependence on ϕ. As the solid particles do not deform, the shear correction factor $\dot{\gamma}_{\mathbf{eff}}/\dot{\gamma}$ is greater than one. It can be shown in the framework of a rigorous upscaling approach to this problem that the optimal estimate of this quantity reads [Chateau *et al.* (2008)]

$$\dot{\gamma}_{\mathbf{eff}}/\dot{\gamma} = \sqrt{(1-\phi)G(\phi)/G(0)} \tag{13}$$

in which the quantity $1 - \phi$ appears because the shear rate experienced by the suspending fluid is linked to the overall shear rate by means of an average equation over the interstitial fluid only. This explains why nonlinear properties cannot depend simply on the reduced solid volume fraction ϕ/ϕ_m.

This approach allows in particular predicting the value $\tau_c(\phi)/\tau_c(0)$ of the dimensionless yield stress of suspensions of noncolloidal particles in yield stress fluids. The apparent viscosity of a perfect plastic yield fluid indeed reads $\tau_c/\dot{\gamma}$. Putting this equation into Eq. 12 combined with Eq. 13 finally yields Eq. 1.

This analysis still allows to physically explain why the relative yield stress increase is lower than the relative elastic modulus increase. Indeed, while the relative apparent viscosity of the suspension is equal to its relative elastic modulus, the shear rate experienced by the suspending fluid is greater than the overall shear rate prescribed to the suspension. As the apparent viscosity of a perfect yield stress fluid is a decreasing function of the shear rate, the localization of the shear rate lowers the consolidating effect of adding solid particles.

We have plotted in Fig. 8 the dimensionless yield stress $\tau_c(\phi, \lambda, \xi)/\tau_c(0) - 1$ as a function of the dimensionless quantity $\sqrt{(1 - \phi)G'(\phi, \lambda, \xi)/G'(0)} - 1$ in logarithmic coordinates for all the systems we studied in order to check that Eq. 1 is still valid. We observe an excellent agreement between our experimental results and the micromechanical estimate Eq. 1 (which is plotted as a straight line $y = x$ in these coordinates).

These results show that the experimental data are consistent with the hypothesis that a uniform estimate of the strain rate over the suspending fluid domain allows to accurately estimate the overall yield stress of a bidisperse suspension from its overall elasticity.

C   Yield stress

Putting the estimate Eq. 10 for the overall linear properties of the suspension into Eq. 1 yields the estimate for the overall yield stress of the suspension:

$$\tau_c(\phi, \lambda, \xi)/\tau_c = \sqrt{(1 - \phi)(1 - \phi/\phi_m)^{-1.43}} \tag{14}$$

We have plotted in Fig. 9 the experimental dimensionless yield stress $\tau_c(\phi, \lambda, \xi)/\tau_c(0) - 1$ as a function of the dimensionless quantity $\sqrt{(1 - \phi)(1 - \phi/\phi_m)^{-1.43}} - 1$ in logarithmic coordinates
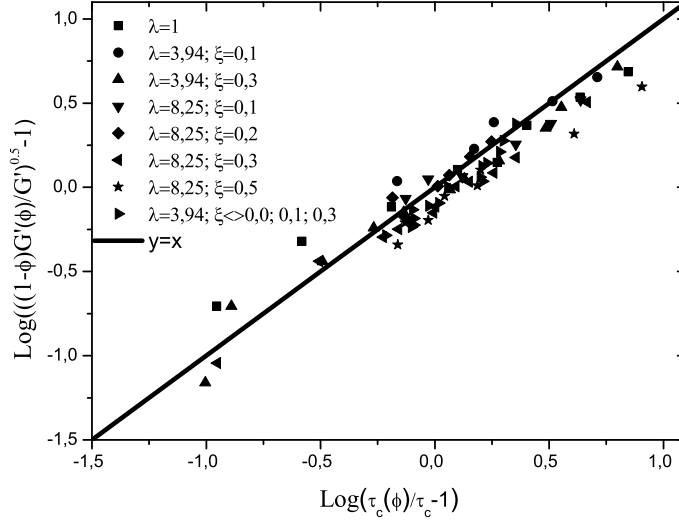
Figure 8: Dimensionless yield stress $\tau_c(\phi, \lambda, \xi)/\tau_c(0)$ as a function of $\sqrt{(1-\phi)G'(\phi, \lambda, \xi)/G'(0)}$ for all the bidisperse suspensions studied (**all particle size ratio λ and fine particle proportion ξ**). The figure's coordinates were chosen so that the $y = x$ line represents the theoretical relation Eq. 1.

for all the systems we studied in order to check that Eq. 14 accurately describes the experimental data.

Even if the fit is not perfect, it is believed that Eq. 14 is accurate enough to predict the yield stress of the bidisperse suspensions studied in this paper.

In order to compare the accuracy of Eq. 14 as an estimate of the overall yield stress of the suspensions with the accuracy of the elastic modulus estimate Eq. 10, we have plotted in Fig. 10 the experimental dimensionless elastic modulus as a function of $(1 - \phi/\phi_m)^{-1.43}$.

At first sight, both estimates seem to accurately fit the experimental data. **To quantitatively assess this point, we have computed the least square error for both the dimensionless yield stress (Fig. 9) and dimensionless elastic modulus (Fig. 10). For quantity y the least square error reads**

$$\mathbf{Err}_y = \frac{1}{N} \sum_{i=1}^{N} \left(y_i^{\mathbf{exp}} - y_i^{\mathbf{th}} \right)^2 \tag{15}$$

with N, the number of measured points, $y_i^{\mathbf{exp}}$, the ith experimentally measured point and $y_i^{\mathbf{th}}$ the associated theoretical value. We found $\mathbf{Err}_G = 0.0071$ for the elastic modulus estimate and $\mathbf{Err}_{\tau_c} = 0.018$ for the yield stress estimate. Both computed
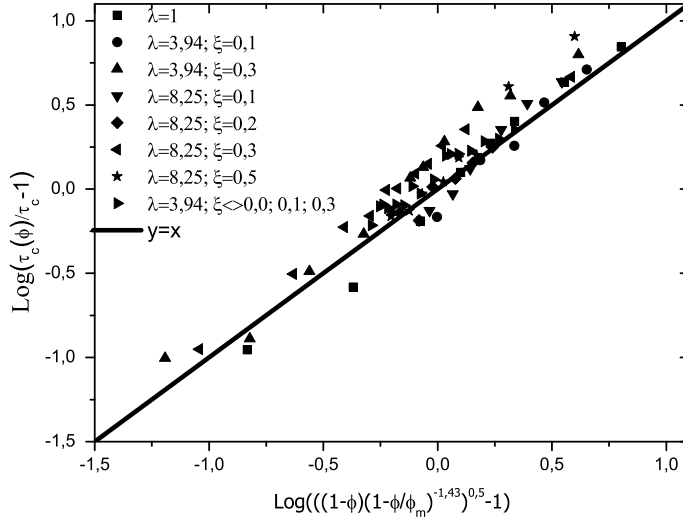
Figure 9: Dimensionless yield stress $\tau_c(\phi, \lambda, \xi)/\tau_c(0)$ as a function of $\sqrt{(1-\phi)(1-\phi/\phi_m)^{-1.43}}$ for all the bidisperse suspensions studied **(all particle size ratio λ and fine particle proportion ξ)**. The figure's coordinates were chosen so that the $y = x$ line represents the theoretical relation Eq. 14.
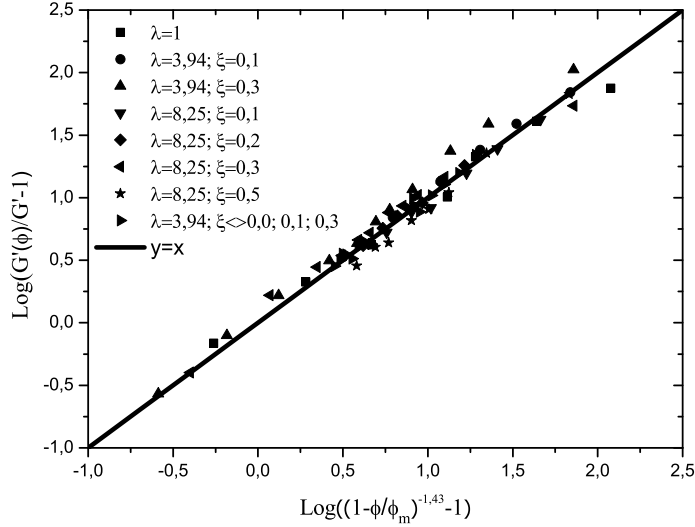

Figure 10: Dimensionless elastic modulus $G'(\phi, \lambda, \xi)/G'(0)$ as a function of $(1 - \phi/\phi_m)^{-1.43}$ for all the bidisperse suspensions studied **(all particle size ratio λ and fine particle proportion ξ)**. The figure's coordinates were chosen so that the $y = x$ line represents the theoretical relation Eq. 10.

23

errors being of the same order of magnitude, it can be concluded that the yield stress estimate Eq.14 is quite as precise than the elastic modulus estimate Eq. 10.

VI   Conclusion

We have studied the elastic modulus and yield stress of an isotropic bidisperse suspension of noncolloidal particles in a yield stress fluid. We focused on the purely mechanical contribution of the noncolloidal particles to the overall properties of the yield stress fluid. To do this, we used materials and procedures designed by Mahaut *et al.* (2008a) to study the case of monodisperse suspensions. We observed that, as it is classically observed for particles suspended in a Newtonian fluid, the elastic modulus and yield stress of bidisperse suspensions are lower than the same quantities measured for monodisperse suspension of same solid volume fraction. We showed that the equation $\tau_c(\phi, \lambda, \xi)/\tau_c(0) = \sqrt{(1-\phi)G'(\phi)/G'(0)}$ of Chateau *et al.* (2008) linking the overall yield stress, the overall elastic modulus and the solid volume fraction still applies when bidisperse suspensions are considered. Additionally, we showed that the effect of the particle size heterogeneity onto the overall rheological properties of the yield stress suspension can be described by means of a packing model developed to estimate random loose packing of assemblies of dry particles. We have finally proposed closed form estimates for both the elastic modulus and the yield stress. This shows that it is sufficient to determine ϕ_m and the dependence of the rheological properties on ϕ to predict the behavior of bidisperse suspensions; this should remain true for more complex polydisperse cases. An extension of this study to the cases of anisotropic particle distribution and more complex polydisperse suspensions is planned for the future.

References

Ancey, C. and H. Jorrot, "Yield stress for particle suspensions within a clay dispersion," J. Rheol. **45**, 297–319 (2001).

Ben Aïm, R., and P. Le Goff, "Effet de paroi dans les empilement désordonnées de sphères et application à la porosité de mélange binaires," Power Technology **1**, 281-290 (1967).

Bournonville, B., P. Coussot, and X. Chateau, "Modification du modèle de Farris pour la prise en compte des interactions géométriques d'un mélange polydisperse de particules," Rhéologie Vol. **7**, 1-8 (2004).

Chang, C., and R. L. Powell, "Effect of particle size distribution on the rheology of concentrated bimodal suspensions," J. Rheol. **38**, 85-98 (1994).

Chateau, X., G. Ovarlez, and K. Luu Trung, "Homogenization approach to the behavior of suspensions of noncolloidal particles in yield stress fluids," J. Rheol. **52**, 489-506 (2008).

Chong, J. S., E. B. Christiansen, and A. D. Baer, "Rheology of concentrated suspensions," J. Appl. Polym. Sci. **15**, 2007-2021 (1971).

Coussot, P., *Rheometry of Pastes, Suspensions and Granular Materials* (John Wiley & Sons, New York, 2005).

Cumberland, D. J., and R. J. Crawford, *The packing of particles, Handbook of Powder Technology, Vol. 6*, (Elsevier, Amsterdam, 1987).

Dodds, J. A., "The porosity and contact points in multicomponent random sphere packings calculated by a simple statistical geometric model," J. Colloid Interface Sci. **77**, 317-327 (1980).

Dong, K. J., R. Y. Yang, R. P. Zou, and A. B. Yu, "Role of the interparticle forces in the formation of random loose packing", Phys. Rev. Lett. **96**, 145505 (2006).

Einstein, A., "Eine neue bestimmung der moleküldimensionen," Ann. Phys. **19**, 289-306 (1906).

Farris, K. J., "Prediction of the Viscosity of Multimodal suspension from Unimodal Viscosity Data," Trans. Soc. Rheol. **12**, 281-301 (1968).

N. A. Frankel and A. Acrivos. On the viscosity of a concentrated suspension of solid spheres. *Chem. Eng. Sci.* 22, 847–853 (1967).

Geiker, M.R., M. Brandl, L. N. Thrane, and L. F. Nielsen. "On the effect of coarse aggregate fraction and shape on the rheological properties of self-compacting concrete," Cement, Concrete and Aggregates **24**, 3–6 (2002).

Gondret, P., and L. Petit, "Dynamic viscosity of macroscopic suspensions of bimodal sized solid spheres," J. Rheol. **41**, 1261-1274 (1997).

Hashin, Z., and S. Shtrikman, "A variational approach to the theory of the elastic behaviour of multiphase materials," J. Mech. Phys Solids **11**, 127-140 (1963).

Krieger, I. M., and T. J. Dougherty, "A Mechanism for Non-Newtonian Flow in Suspensions of Rigid Sphere," Trans. Soc. Rheol. **3**, 137-152 (1959).

de Larrard, F., T. Sedran, and D. Angot, "Prévision de la compacité des mélanges granulaires par le modèle de suspension solide I-fondements théoriques et étalonnage du modèle," Bull. liaison Labo. P. et Ch., 59-70 (1994).

de Larrard, F., T. Sedran, and D. Angot, "Prévision de la compacité des mélanges granulaires par le modèle de suspension solide II-validation Cas des mélanges confinés," Bull. liaison Labo. P. et Ch., 71-86 (1994).

de Larrard, F., *Concrete Mixture Proportioning: a scientific approach* (E & FN Spon, 1999)

Larson, R. G., *The structure and Rheology of Complex fluids* (Oxford University Press, New York, 1999).

Mahaut, F., X. Chateau, P. Coussot, and G. Ovarlez, "Yield stress and elastic modulus of suspensions of noncolloidal particles in yield stress fluids," J. Rheol. **52**, 287-313 (2008).

Mahaut, F., S. Mokéddem, X. Chateau, N. Roussel, and G. Ovarlez, "Effect of coarse particle volume fraction on the yield stress and thixotropy of cementious materials," Cement and Concrete Research **38**, 1276-1285 (2008).

Neville A. M, *Properties of Concrete* 3rd edition (Pitman, 1981).

Onoda G., and E. G. Liniger, "Random loose packings of uniform spheres and the dilatancy onset," Phys. Rev. Lett. **64**, 2727-2730 (1990).

G. Ovarlez, F. Bertrand, and S. Rodts, "Local determination of the constitutive law of dense suspension of noncolloidal particles through magnetic resonance imaging," J. Rheol. **50**, 259-292 (2006).

G. Ovarlez, Q. Barral, and P. Coussot, "Three-dimensional jamming and flows of soft glassy materials," Nature Materials **9**, 115-119 (2010).

Phan-Thien, N., and D. C. Pham, "Differential multiphase models for polydispersed suspensions and particulate solids," J. Non-Newtonian Fluid Mech. **72**, 305-318 (1997).

Probstein, R. F., M. Z. Sengun, and T. -C. Tseng, "Bimodal model of concentrated suspension viscosity for distributed particle sizes," J. Rheol. **38**, 811-829 (1994).

Servais, C., R. Jones, and I. Roberts, "The influence of particle size distribution on the processing of food," J. food Eng. **51**, 201-208 (2002).

Shapiro, A. P., and R. F. Probstein, "Random packing of spheres and fluidity limits of monodisperse and bidisperse suspensions," Phys. Rev. Lett. **68**, 1422-1425 (1992).

Stickel, J. J., and R. L. Powell, "Fluid mechanics and rheology of dense suspensions," Annu. Rev. Fluid. Mech. **37**, 129-149 (2005).

Storms, R. F., B. V. Ramarao, and R. H. Weiland, "Low shear rate viscosity of bimodally dispersed suspensions," Power Technology **63**, 247-259 (1990).

Stovall, T., F. de Larrard, and M. Buil, "Linear Packing density model of grains mixtures," Power Technology **48**, 1 (1986).

Stovall, T., M. Buil, and Ch. Such, "Viscosité des suspensions multimodales," Journées Physique - Les milieux granulaires, 73-78 (1987).